



PII S0016-7037(00)00775-X

Extent of intermixing among framework units in silicate glasses and melts

S. K. LEE^{1,*} and J. F. STEBBINS¹¹Department of Geological and Environmental Sciences, Stanford University, Stanford, CA 94305 USA

(Received March 30, 2001; accepted in revised form July 13, 2001)

Abstract—One aspect of the inherent disorder in silicate glasses and melts is the intermixing among framework units, which has important implications to the macroscopic properties of silicate magmas. We present experimental evidence of extensive mixing of these framework units in silicate glasses including aluminosilicate and borosilicate glasses from oxygen-17 nuclear magnetic resonance (NMR), which shows remarkable similarity to predictions from ab initio molecular orbital calculations. We quantify the extent of framework disorder by introducing the degree of interdispersion (P) ranging from complete phase separation to random distribution for borosilicate glasses and the degree of Al avoidance (Q) for aluminosilicate glasses. Boron-11 triple quantum magic angle spinning NMR results show that the fraction of the boroxol ring group increases with increasing boron content in binary borosilicate glasses, affecting the corresponding configurational enthalpy. We demonstrate that a more complete description of the macroscopic thermodynamic properties of silicate glasses can be successfully derived from detailed information on the degree of framework disorder. Copyright © 2002 Elsevier Science Ltd

1. INTRODUCTION

Silicate glasses, including borosilicates and aluminosilicates and their precursor liquids, have long been studied because of their diverse applications in the glass industry (Dell et al., 1983; Youngman et al., 1995) and the implications of their structures to the properties and dynamics of silicate magmas (Mysen et al., 1982; Stebbins and Xu, 1997). These glasses, as covalent random networks, have well-defined nearest-neighbor atomic environments forming corner-sharing framework units such as SiO_4 or AlO_4 tetrahedra (^{29}Si and ^{27}Al) (Engelhardt and Michel, 1987) and three- or four-coordinated BO_3 or BO_4 groups (^{11}B and ^{10}B) linked by bridging oxygens (Dell et al., 1983). The local configurations of these framework units (a key aspect of the short-range order) have major effects on the transport properties, including viscosity and diffusivity, and on the thermodynamic properties and phase relations of the melts, such as configurational entropy, heat capacity, and activity coefficients (Navrotsky et al., 1982; Richet et al., 1997; Mysen, 1998; Lee and Stebbins, 1999, 2000a,b). In spite of its importance, quantitative estimation of the extent of the inherent disorder in silicate glasses and melts has remained a complex and difficult problem, largely because of the limits of resolution of conventional experimental techniques. For example, exploration of the distribution of Si and Al within the network has been hampered by their similar atomic scattering factors (Petkov et al., 2000). Conventional magic angle spinning (MAS) solid-state nuclear magnetic resonance (NMR) has proved of limited utility for determining the local arrangement of framework units due to the lack of resolution caused by chemical shift distributions and quadrupolar broadening (Lee and Stebbins, 2000b). On the other hand, recent development of triple quantum (3Q) MAS NMR has offered improved resolution, free from quadrupolar broadening for nuclides such as ^{27}Al and ^{17}O (Baltisberger et al., 1996; Lee and Stebbins, 2000b). In

particular, ^{17}O 3QMAS NMR yields information on the oxygen site configurations in oxide glasses and their relative populations, scaled by the 3QMAS efficiency, which in turn is dependent on one of the structurally relevant parameters, the quadrupolar coupling constant (C_q). This method has become especially useful in the investigation of framework disorder, allowing this important aspect of degree of randomness in oxide glasses to be evaluated (Lee and Stebbins, 1999, 2000a).

In our recent studies of aluminosilicate glasses, which represent the predominant types of magmas in the Earth's upper mantle and crust, we used the degree of "aluminum avoidance" (Q) to quantify the extent of framework disorder, which has been an important problem in high-temperature geochemistry for decades (Lee and Stebbins, 1999). In contrast, borosilicates are one of the most important types of technological glass-forming systems and have growing applications in nuclear waste storage. Borosilicate glasses in the B_2O_3 - SiO_2 binary, which can serve as a model system for the more complex compositions, have been of particular interest because of the fundamental implications of the degree of mixing between the silicate network (^{29}Si) and that composed of three-coordinated boron (^{11}B), leading to controversies on phase separation and inherent spatial inhomogeneity (Porai-Koshits and Wright, 1996; Wright et al., 1996).

Successful boron speciation models for ternary borosilicate glasses based on ^{11}B NMR (Dell et al., 1983) postulate no structural units made of both ^{29}Si and ^{11}B and thus imply low probability for the intermixing of these framework units. The formation of oxygen clusters connecting ^{29}Si and ^{11}B (^{29}Si - O - ^{11}B) in binary borosilicate glasses has been thought to be limited, as suggested by calculated glass immiscibility that propagates into ternary systems and by the positive heat of mixing from solution calorimetry (Charles and Wagstaff, 1968; Hervig and Navrotsky, 1985). However, clear evidence of mixing between the two units has been reported in recent ^{17}O and ^{11}B NMR studies (Wang and Stebbins, 1998; Sorarú et al., 1999), suggesting instead a random distribution of framework

* Author to whom correspondence should be addressed (sklee@pangea.stanford.edu).

units (Martens and Müller-Warmuth, 2000). Therefore, it is of crucial importance to provide a quantitative assessment of the extent of B-Si disorder. ^{11}B 3QMAS NMR is also an important tool to provide the information on the local configurations, including the variation of boroxol ring content with composition and its effect on the material properties (Hwang et al., 1997).

Here, we report ^{17}O and ^{11}B 3QMAS NMR spectra for binary borosilicate glasses and a ^{17}O 3QMAS NMR spectrum for a calcium aluminosilicate glass. We describe a general framework for exploring the degree of disorder in silicate glasses by the introduction of the “degree of aluminum avoidance” in aluminosilicate glasses and the “degree of interdispersion (degree of phase separation)” in borosilicate glasses, the latter ranging from complete phase separation to random distribution. We also quantify the extent of intermixing among the network units in these glasses via ^{17}O NMR and ab initio molecular orbital calculations combined with statistical thermodynamic modeling.

2. EXPERIMENTAL

Binary borosilicate glass samples are synthesized as previously described (Wang and Stebbins, 1998; Lee et al., in press) from ^{17}O -enriched SiO_2 and B_2O_3 with nominal compositions of $\text{B}_2\text{Si}_{2R}\text{O}_{3+4R}$, where R ($=\text{Si/B}$) is 2 (sample BS28), 0.75 (BS46), and 0.33 (BS64). ^{17}O -enriched boron and silicon oxides were prepared by hydrolyzing silicon tetrachloride and boron trichloride in 45% ^{17}O -enriched water. B_2O_3 glass was prepared by melting B_2O_3 reagent. ^{17}O -enriched Ca-aluminosilicate glass with a nominal composition of $\text{CaAl}_2\text{SiO}_6$ was synthesized at 1873 K from CaCO_3 , Al_2O_3 , and ^{17}O -enriched SiO_2 as previously described (Stebbins et al., 1999b).

^{17}O 3QMAS spectra for binary borosilicate glasses were collected at a Larmor frequency of 54.2 MHz (9.4 T) with the shifted-echo pulse sequence with two hard pulses of durations of 5.3 μs and 1.8 μs , respectively, and a selective pulse with duration of 26 μs applied after n rotor cycles, or ~ 0.5 ms (Baltisberger et al., 1996; Lee and Stebbins, 2000b). The spin-lattice relaxation time for each sample was measured with the saturation-recovery method, and the delay times were chosen to be three times T_1 , typically 1 to 4 s. Spinning speed was 15 kHz, and all spectra are referenced to external tap water. The 3QMAS spectrum of calcium aluminosilicate glass was obtained as described above except with a recycle delay 12 s and a delay between second and third pulse of ~ 0.5 ms. ^{11}B 3QMAS NMR spectra for binary borosilicate glasses and B_2O_3 glass were collected on a Varian Inova 600 spectrometer at a Larmor frequency of 192.42 MHz and a spinning speed of 18 kHz with a 3.2-mm Varian/Chemagnetic MAS probe. The shifted-echo pulse sequence comprising two hard pulses of duration 3.5 μs and 1.2 μs , and a selective pulse with duration of 20 μs and an echo time of 2 ms was used. The spectra were referenced to $\text{BF}_3(\text{CH}_3\text{CH}_2)_2\text{O}$, which resonates at -19.6 ppm with respect to the observed 1 M boric acid (H_3BO_3) solution.

3. RESULTS AND DISCUSSION

3.1. ^{17}O and ^{11}B 3QMAS Spectra for Binary Borosilicates

Figure 1 illustrates the ^{17}O 3QMAS NMR spectra of binary borosilicate glasses with varying Si/B ratios, where three bridging oxygen sites $^{[4]}\text{Si-O-}^{[4]}\text{Si}$, $^{[3]}\text{B-O-}^{[3]}\text{B}$, and especially $^{[4]}\text{Si-O-}^{[3]}\text{B}$ are clearly resolved for all Si/B ratios. The area fraction of the isotropic projection for each oxygen cluster can be regarded as the true oxygen site population because C_q for each cluster, the dominant factor for 3QMAS efficiency, is similar (5.5 to 5.9 MHz) (Wang and Stebbins, 1998). C_q and the isotropic chemical shifts (δ_{iso}) are rather similar throughout the

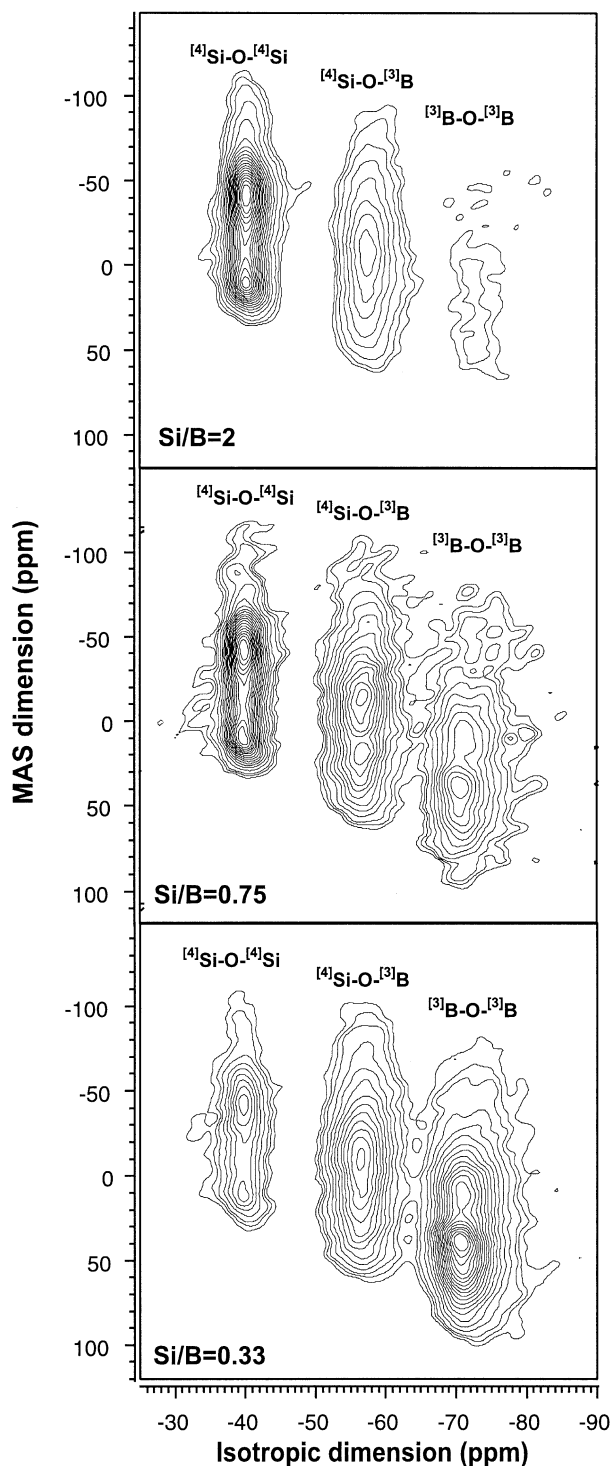


Fig. 1. ^{17}O 3QMAS NMR spectra for binary borosilicate glasses with varying Si/B. Contour lines are drawn from 4 to 99 % of relative intensity with a 5 % increment and added line at the 6.5 % level to better show low-intensity peaks.

binary because of the lack of charge balancing or modifying cations. These are among the major sources of C_q variation for bridging oxygen sites, as has been demonstrated in aluminosilicate glasses, where δ_{iso} also increases with decreasing Si/Al

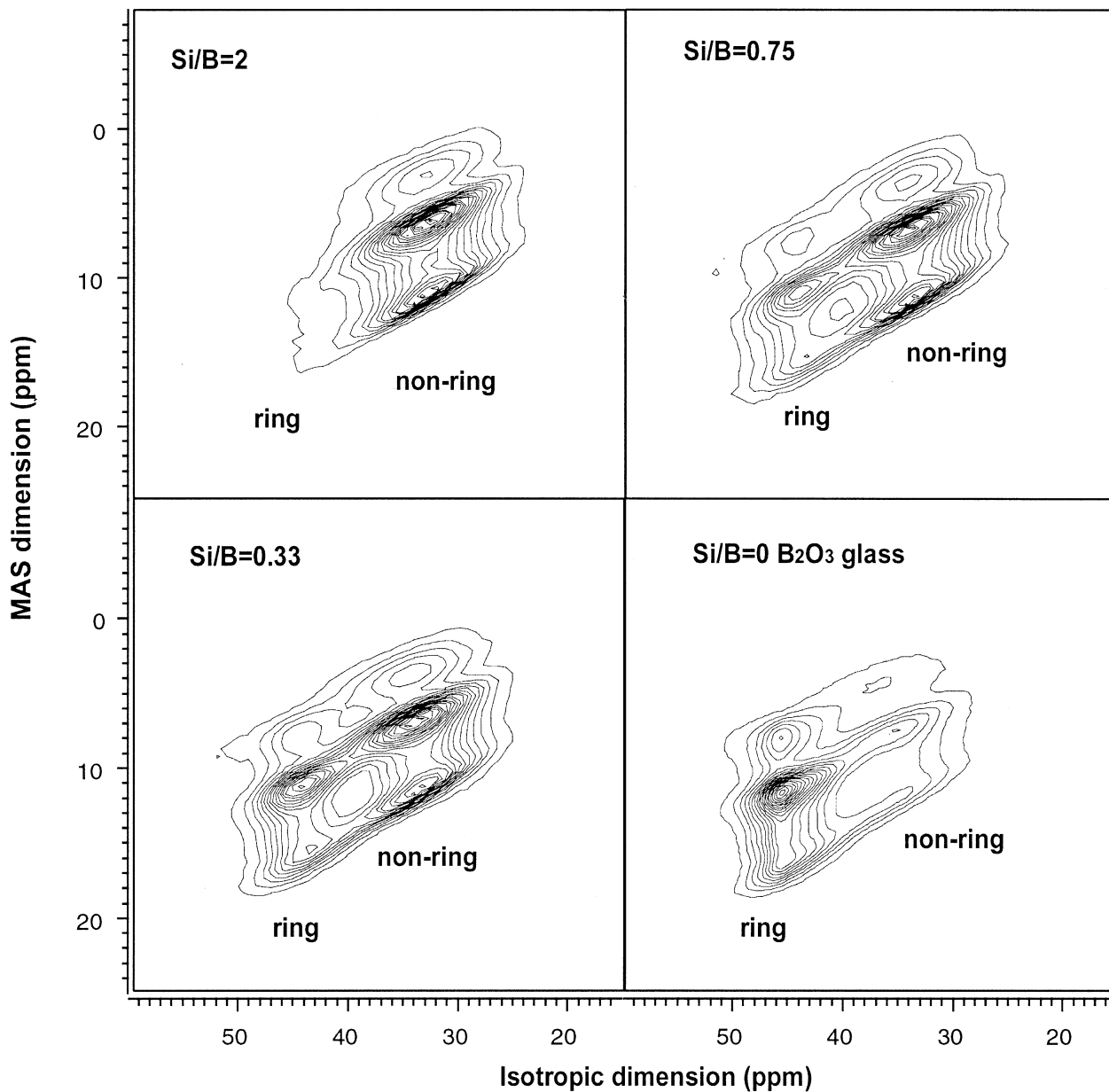


Fig. 2. ^{11}B 3QMAS NMR spectra of binary borosilicate glasses and B_2O_3 glass with varying Si/B. Contour lines are drawn from 3 to 98% of relative intensity with a 5% increment.

ratio and thus increasing Na content (Lee and Stebbins, 2000b). The fraction of $^{[4]}\text{Si-O-}^{[4]}\text{Si}$ increases with increasing silica content, whereas that of $^{[3]}\text{B-O-}^{[3]}\text{B}$ decreases. The large fraction of $^{[4]}\text{Si-O-}^{[3]}\text{B}$ for all three samples demonstrates that phase separation is not prominent, allowing considerable mixing among the framework units.

Figure 2 shows the ^{11}B 3QMAS NMR spectra of the binary borosilicate glasses. Two clearly resolved structural components are assigned as boron in boroxol rings (consisting of three corner shared BO_3 triangles) and boron in nonring sites (Lee et al., in press). C_q of each site, obtained from the center of gravity of each peak, slightly increases with increasing Si content from $2.75 (\pm 0.1)$ (BS28) to $2.92 (\pm 0.05)$ MHz (B_2O_3)

for the nonring component and $2.70 (\pm 0.1)$ (BS28) to $2.82 (\pm 0.05)$ MHz (B_2O_3) for the ring component. These values—in particular that for B_2O_3 —are somewhat larger than those derived from ^{11}B MAS NMR partly because of the uncertainties caused by peak overlap in ^{11}B 3QMAS NMR spectra (Lee et al., in preparation). δ_{iso} decreases with increasing Si/B ratio from $12.6 (\pm 0.5)$ (BS28) to $13.9 (\pm 0.5)$ ppm (B_2O_3) for nonring component and from $15.8 (\pm 1)$ (BS28) to $17.9 (\pm 0.5)$ ppm (B_2O_3), implying increased shielding with increasing Si around B. These results show good agreement with our recent ^{11}B MAS NMR results and imply that both boroxol ring and nonring components bond with SiO_4 group.

The fraction of the boroxol ring component increases with

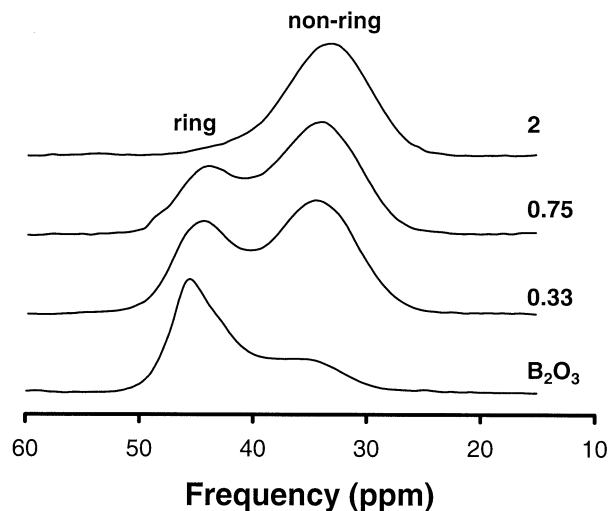


Fig. 3. Total projections in the isotropic dimension of ^{11}B 3QMAS spectra for binary borosilicate glasses and B_2O_3 glass with varying Si/B as labeled.

increasing boron content in binary borosilicate glasses as shown in isotropic projections of ^{11}B 3QMAS spectra (Fig. 3), which is consistent with results from our recent ^{11}B MAS NMR spectra. On the other hand, the fraction of the boroxol rings from 3QMAS is smaller than that obtained from ^{11}B MAS NMR: in BS64, fraction of boroxol rings from ^{11}B MAS NMR is $\sim 48\%$ compared with 38% from 3QMAS NMR (Lee et al., in press). This discrepancy may be due to the small C_q difference between two components where the boroxol ring has larger C_q than nonring component, affecting 3QMAS efficiency or to slight differential relaxation between the two boron sites. It should also be noted that the calculation of the boron site fraction from ^{11}B MAS NMR by simulating the spectra may also introduce uncertainty.

3.2. Extent of Disorder and Configurational Thermodynamic Properties in Silicate Glasses: Theory and Applications

The population of each bridging oxygen can provide explicit information on the degree of interdispersion among units and can be obtained from the following relations, considering the difference in coordination number of each unit as a function of fictive temperature and of composition (Lee and Stebbins, 1999):

$$X_{\text{B-O-Si}} = 4X_{\text{B}}'X_{\text{Si}}' \left(\frac{1}{\beta + 1} \right), \quad (1)$$

where $\beta = \sqrt{1 + 4X_{\text{Si}}'X_{\text{B}}' \{ \exp[2W/kT_f(X_{\text{Si}})] - 1 \}}$, $X_{\text{Si}}' = z_{\text{Si}} X_{\text{Si}} / (z_{\text{Si}} X_{\text{Si}} + z_{\text{B}} X_{\text{B}})$, and $X_{\text{B}}' = z_{\text{B}} X_{\text{B}} / (z_{\text{Si}} X_{\text{Si}} + z_{\text{B}} X_{\text{B}})$ refer to the normalized mole fraction of Si and B. X_{Si} and X_{B} are the mole fractions of Si and B relative to total (Si + B), and z_{Si} and z_{B} are the coordination numbers of Si and B, respectively. $2W$ is the cluster energy difference in the reaction $[^{14}\text{Si-O-}^{14}\text{Si}] + [^{13}\text{B-O-}^{13}\text{B}] = 2[^{14}\text{Si-O-}^{13}\text{B}]$. k is the Boltzmann constant and $T_f(X_{\text{Si}})$ is the composition-dependent fictive temperature at which the equilibrium liquid structure is quenched into the glass. Here,

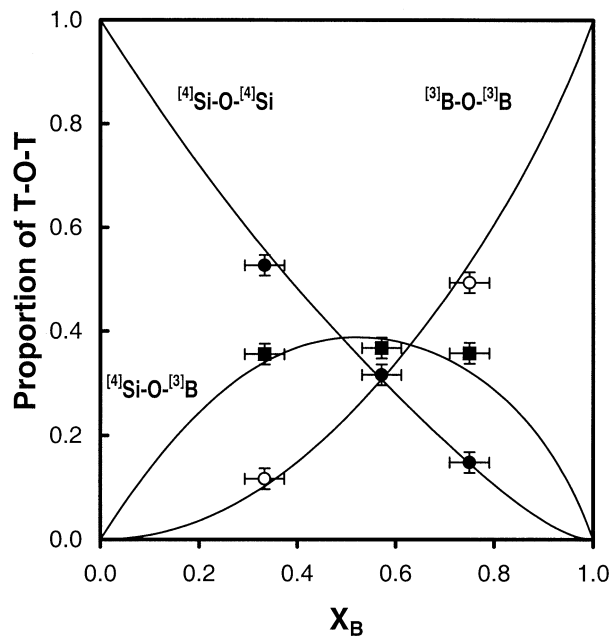


Fig. 4. Variation in oxygen-site populations in binary borosilicate glasses with X_{B} (mole fraction of boron relative to B + Si). Solid circles and squares refer to the experimental oxygen site populations (from ^{17}O 3QMAS NMR) of $^{14}\text{Si-O-}^{14}\text{Si}$ and $^{14}\text{Si-O-}^{13}\text{B}$, and open circles show experimental fraction of $^{13}\text{B-O-}^{13}\text{B}$. The solid lines represent the calculated oxygen site populations with $2W = 5.4$ kJ/mol.

the cluster energy difference ($2W$) controls the relative population of each cluster and can be evaluated directly from ab initio molecular orbital calculations. The clear experimental evidence of framework mixing can be quantified by the introduction of the degree of interdispersion (P), where $p = 1$ refers to the complete phase separation (giving rise to negligible $^{14}\text{Si-O-}^{13}\text{B}$) and $P = 0$ represents random mixing among framework units, which would yield 50% of $^{14}\text{Si-O-}^{13}\text{B}$ for BS46. Here, the degree of interdispersion (the degree of phase separation, P) among network units is defined as

$$P = 1 - \exp[-(2W/kT_f(X_{\text{Si}}))], \quad (2)$$

where the definitions of the variables are given previously. The degree of interdispersion also changes with composition due to the composition-dependent fictive temperature. The variation of experimental oxygen site populations with composition agrees well with the calculated values (Eqn. 1) with $P \approx 0.62$ ($2W = 5.4$ kJ/mol) at BS46 as illustrated in Figure 4, confirming the prediction of considerable network mixing but clearly not fully random. These results are also remarkably similar to the prediction obtained from the recent quantum chemical calculations based on density functional theory where the calculated $2W$ is ~ 5.8 kJ/mol (Frisch et al., 1998; Lee et al., in press). Here, $2W$ was calculated at the B3LYP/6 to 311G(2d,p) level for clusters such as $^{14}\text{Si-O-}^{13}\text{B}$ ($(\text{Si}(\text{OH})_3\text{-O-B}(\text{OH})_2)$), $^{14}\text{Si-O-}^{14}\text{Si}$ ($(\text{OH})_3\text{Si-O-Si}(\text{OH})_3$), and $^{13}\text{B-O-}^{13}\text{B}$ ($(\text{OH})_2\text{B-O-B}(\text{OH})_2$), which were fully optimized at the HF/3-21G level with Gaussian98.

Framework mixing in alkali aluminosilicate glasses has been recently quantified in terms of the degree of Al avoidance,

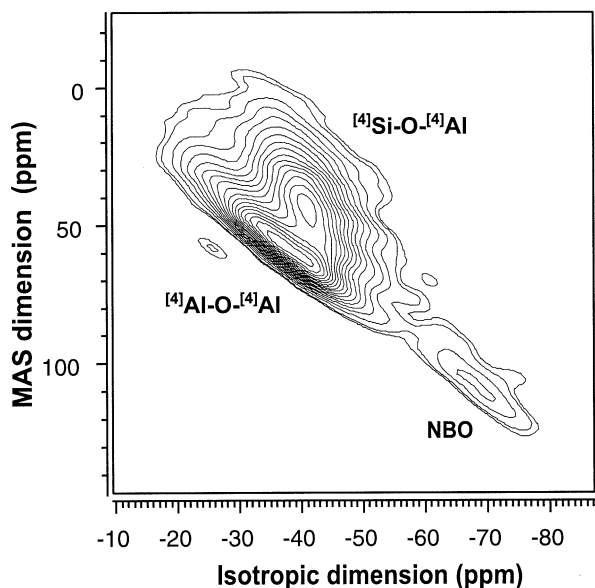


Fig. 5. ^{17}O 3QMAS spectrum of $\text{CaAl}_2\text{Si}_2\text{O}_8$ glass collected at 9.4 T. Contour lines are drawn from 9 to 99 % of relative intensity with a 5 % increment and an added line at the 7 % level.

demonstrating that the Al avoidance is imperfect, leading to $\sim 10\%$ of $^{[4]}\text{Al-O-}^{[4]}\text{Al}$ in NaAlSiO_4 glasses. In such systems, most or all the polyhedral units are four-coordinated—that is, $^{[4]}\text{Si}$ and $^{[4]}\text{Al}$ (Lee and Stebbins, 2000a,b). On the other hand, recent results for charge-balanced calcium aluminosilicate glasses from high-energy X-ray diffraction report that the formation of nonbridging oxygen is associated with the decrease of coordination around Si to less than four for $\text{Si/Al} < 1$ glasses (Petkov et al., 1998, 2000). This report may not explain the formation of nonbridging oxygen in high silica aluminosilicate glasses. Oxygen NMR and oxygen site statistics developed here give a more direct insight into the site connectivity and cation coordination in aluminosilicate glasses. Figure 5 shows ^{17}O 3QMAS NMR spectrum of a charge-balanced Ca-aluminosilicate glass with $\text{Si/Al} = 0.5$. The isotropic projection of the 3QMAS spectrum was fitted with two gaussian components representing $^{[4]}\text{Al-O-}^{[4]}\text{Al}$ and $^{[4]}\text{Si-O-}^{[4]}\text{Al}$. The peak positions ($\delta_{3\text{QMAS}}$) were constrained to vary around -34 ± 0.5 ppm for the former and -41 ± 0.5 ppm for the latter. $^{[4]}\text{Al-O-}^{[4]}\text{Al}$ and $^{[4]}\text{Si-O-}^{[4]}\text{Al}$ peaks are partially resolved, and the populations of the clusters are $\sim 38 \pm 5\%$ and $62 \pm 5\%$, respectively, considering the C_q dependence of 3QMAS efficiency. Such a level of quantification was not reached in our previous report on Ca-aluminosilicate glasses due to a lower resolution (Stebbins et al., 1999a). These experimental results agree well with the prediction from ^{29}Si MAS NMR with a degree of Al

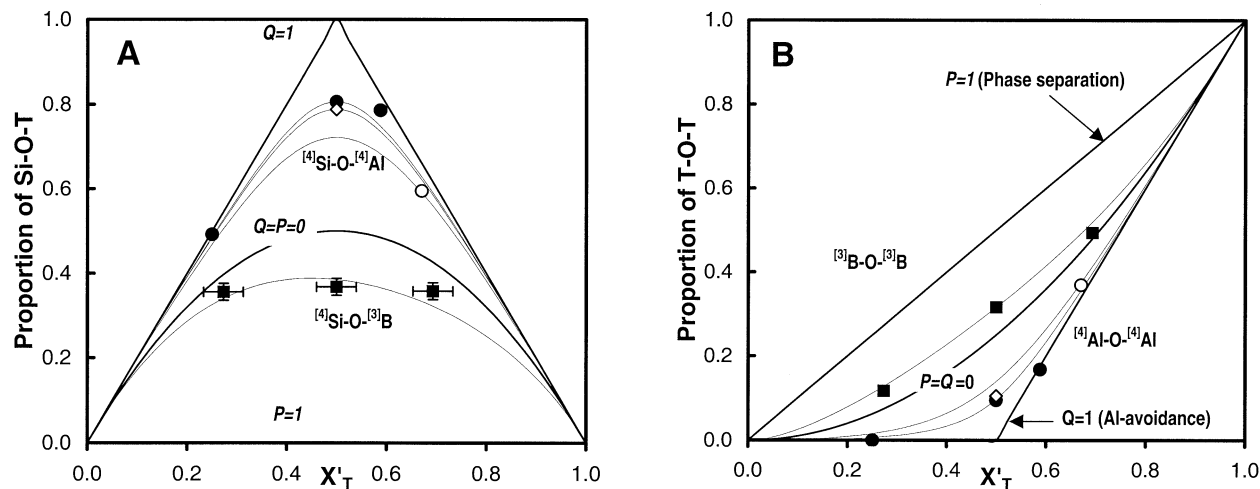


Fig. 6. Oxygen site populations in silicate glasses including aluminosilicate and borosilicate glasses as a function of X'_T , which is the normalized mole fraction of framework cation (e.g., $T = \text{Al}$ or B) as defined in Eqn. 1. (A) Populations of oxygens linking different types of framework units (Si-O-T). Solid circles represent $^{[4]}\text{Si-O-}^{[4]}\text{Al}$ in $\text{SiO}_2\text{-NaAlO}_2$ (Lee and Stebbins, 2000a), and solid squares refer to $^{[4]}\text{Si-O-}^{[3]}\text{B}$ in binary borosilicates (from ^{17}O 3QMAS NMR). Open diamond and open circle show the fraction of $^{[4]}\text{Si-O-}^{[4]}\text{Al}$ in LiAlSiO_4 glass (Lee and Stebbins, 2000a) and $\text{CaAl}_2\text{Si}_2\text{O}_8$ glass, respectively. Thin solid lines show (from upper to lowermost) the calculated oxygen site populations of $^{[4]}\text{Si-O-}^{[4]}\text{Al}$ with Q of 0.942 (for Na-aluminosilicates, Na-AS) (Lee and Stebbins, 2000a), 0.928 (LiAlSiO₄ glass), and 0.85 (for Ca-aluminosilicates, Ca-AS) at 1050 K and $^{[4]}\text{Si-O-}^{[3]}\text{B}$ with P of 0.62 (for binary borosilicate glasses, BS) from the largest Si-O-T. Solid lines are the calculated Si-O-T with Q of 1 and 0. (B) Populations of oxygens connecting the same framework units (T-O-T; e.g., $^{[4]}\text{Al-O-}^{[4]}\text{Al}$ and $^{[3]}\text{B-O-}^{[3]}\text{B}$). Solid circles and squares represent the experimental oxygen site populations for $^{[4]}\text{Al-O-}^{[4]}\text{Al}$ and $^{[3]}\text{B-O-}^{[3]}\text{B}$ in Na-AS and BS, respectively. Open diamond and open circles show the fraction of $^{[4]}\text{Al-O-}^{[4]}\text{Al}$ in LiAlSiO_4 (Lee and Stebbins, 2000a) and $\text{CaAl}_2\text{Si}_2\text{O}_8$ glasses. Thin solid lines show (from lower to uppermost) the calculated oxygen site populations of T-O-T with Q of 0.942 (for Na-AS) (Lee and Stebbins, 2000a), 0.928 (LiAlSiO₄ glass), and 0.85 (for Ca-AS) at 1050 K and $^{[4]}\text{Si-O-}^{[3]}\text{B}$ with P of 0.62 (for BS) from the lowest T-O-T. Solid lines are the calculated T-O-T with Q of 1 (Al avoidance) and 0 (random distribution) and $P = 1$ (complete phase separation) from the lowest. The composition-dependent T_f was used in calculation of $^{[3]}\text{B-O-}^{[3]}\text{B}$ and $^{[4]}\text{Si-O-}^{[3]}\text{B}$ for borosilicate glasses.

avoidance (Q) of around 0.85 where Q varies from 0 (random distribution of framework units) to 1 (complete Al avoidance) based on the constraint of the same coordination number of 4 for Si and Al. The degree of Al avoidance among network units was defined previously (Lee and Stebbins, 1999) and is given as

$$Q = 1 - \exp(2W/kT_i). \quad (3)$$

The results from borosilicates and aluminosilicates can be combined to yield a general framework for understanding the extent of short-range order in silicate glasses. Figure 6 illustrates the variation of oxygen site populations (Si-O-T and T-O-T) in charge-balanced silicate glasses with respect to the degree of intermixing (Q and P) and composition. The latter is represented as the normalized mole fraction (X_T' , where T = B or Al) to facilitate comparison among systems with different coordination numbers. Framework mixing in charge-balanced silicate glasses can thus be quantified from experimental oxygen site populations derived from NMR. The degree of mixing in the binary borosilicates can be seen to lie in the intermediate range between a random distribution and complete phase separation and that of aluminosilicates is constrained to lie in the region between random mixing and strict Al-avoidance (no $^{[4]}\text{Al-O-}^{[4]}\text{Al}$).

The quantification of chemical short-range order has critical implications to configurational thermodynamic properties that in turn are of central importance to activity-composition relations in silicate liquids. We calculate the configurational enthalpy of Ca- and Na-aluminosilicate and binary borosilicate glasses using the statistical thermodynamic modeling and the constraints from NMR and compare the results to heats of mixing derived from solution calorimetry (Fig. 7). Configurational enthalpy due to chemical mixing can be calculated as

$$H^{\text{config}} = \frac{z_{\text{tot}} X_{T1}' X_{T2}'}{\beta + 1} 2W, \quad (4)$$

where $z_{\text{tot}} = z_{T1} X_{T1} + z_{T2} X_{T2}$. T1 and T2 refer to framework cations.

Previously, we have demonstrated that the results from these two methods yield good agreement for aluminosilicate glasses (Navrotsky et al., 1982; Lee and Stebbins, 1999, 2000a,b). For the binary borosilicate glasses, the configurational enthalpy calculated from NMR-derived oxygen site fractions and considering only chemical intermixing (ignoring possible intermediate-range order), shows remarkable similarity to that calculated from quantum simulations with the larger of the two basis set tested (curve b in Fig. 7B). The configurational enthalpy is, however, rather smaller than that from solution calorimetry (Fig. 7B) in compositions with high boron contents. A likely explanation of this discrepancy is inherent topological short-range order or intermediate range order. Particularly important is the formation of boroxol rings, as shown in the Figures 2 and 3 and by our recent ^{11}B MAS NMR spectra where the boroxol ring group increases linearly with increasing boron content from ~17% in BS28 to 70% in B_2O_3 glasses (Lee et al., in press). The extra energy of forming boroxol rings, ~14 kJ/mol, can be estimated by adding a term linear in composition to the configurational enthalpy.

These results show that a considerable fraction of the heat of mixing in binary borosilicate glasses can be due to topological

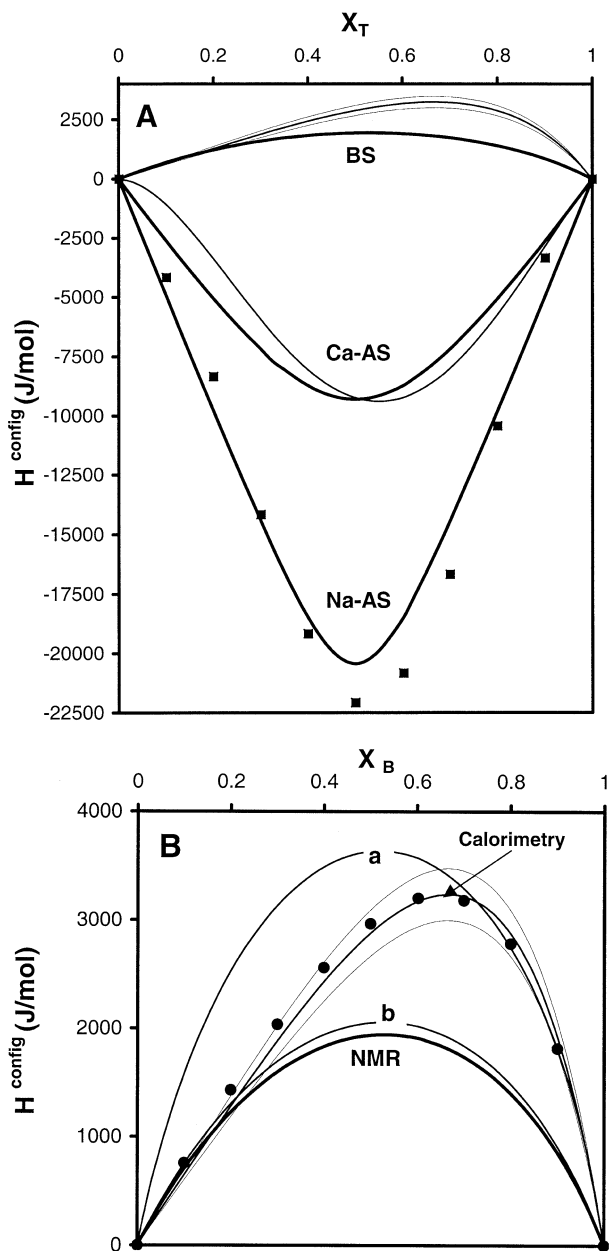


Fig. 7. (A) Configurational enthalpies (H^{config}) of various silicate glasses obtained from ^{17}O NMR and solution calorimetry. X_T is the mole fraction of B or Al. Heavy solid lines represent the calculated configurational enthalpy from ^{17}O NMR at $P = 0.62$ (BS46), $Q = 0.8$ (Ca-AS), and 0.94 (Na-AS) and relationship given in Eqn. 4. Solid lines and solid squares represent the enthalpy of mixing obtained from solution calorimetry (Navrotsky et al., 1982; Hervig and Navrotsky, 1985). BS, Ca-AS, and Na-AS refer to the charge-balanced binary borosilicate glasses ($\text{BO}_{1.5}\text{-SiO}_2$) Ca-aluminosilicate and Na-aluminosilicate glasses, respectively. The uncertainty in the configurational enthalpy from solution calorimetry in the BS system is also shown. (B) Configurational enthalpy for binary borosilicate glasses with mole fraction of boron relative to B + Si. Curves a and b show the results obtained by combining molecular orbital calculations of $2W$ at the B3LYP/6-311G(d)//HF/3-21G level (a) and at the B3LYP/6-311+G(2d,p)//HF/3-21G level (b) with statistical thermodynamic modeling, respectively. Solid circles represent the calculated H^{config} considering the formation of boroxol rings.

contributions, in particular the formation of boroxol rings, and that these effects can be clearly separated. A possible complication to the concept given here is whether ring and nonring boron groups have different degrees of intermixing with ^{14}Si . However, in the limiting cases where boroxol rings are assumed not to mix with ^{14}Si , the experimental oxygen site populations cannot be explained: the maximum $^{14}\text{Si-O-}^{14}\text{Si}$ fraction and minimum $^{13}\text{B-O-}^{13}\text{B}$ fraction in binary borosilicate glasses with $\text{Si/B} = 0.75$ (BS46), which contains $\sim 42\%$ of boroxol ring, are ~ 27 and 47% , respectively, whereas the experimental fractions of these clusters are around 31% each respectively, suggesting that ^{14}Si units are dispersed among both nonring and boroxol ring components. The temperature effect on mixing among framework units in silicate glasses and melts is also of crucial importance, which was predicted and later verified in our recent studies on aluminosilicate glasses and melts (Lee and Stebbins, 1999, 2000a). This effect is considered in our calculations for oxygen site populations and configurational thermodynamic properties of binary borosilicate glasses as explicitly described in Eqn. 1 and Eqn. 4. The extent of intermixing increases with increasing temperature, leading to an increased fraction of $^{14}\text{Si-O-}^{13}\text{B}$ or $^{14}\text{Si-O-}^{14}\text{Al}$, which reduces the configurational heat capacity stemming from chemical mixing among the networks. This result may account for the trend in configurational heat capacities for alkali titanosilicates and binary borosilicates melts obtained from solution calorimetry that show negative temperature dependence (Bouhifd et al., 1999).

In this study, we shed light on the prediction and quantification of the degree of chemical short-range order using NMR and ab initio molecular orbital calculations combined with statistical thermodynamics. We also demonstrated that relatively complete descriptions of the ambient pressure macroscopic thermodynamic properties of a simple silicate glass system can be derived from detailed experimental information on the degree of disorder. This approach offers improved prospects for quantifying other aspects of the extent of disorder in silicate glasses including topological disorder as exemplified by bond angle distribution functions (Lee et al., in press). Furthermore, the kinetic stability of silicate glasses and melts in contact with water should also depend on the framework disorder because the reactivity of each oxygen cluster with H_2O is different (Stebbins et al., 1999b). Finally, the method and results given here have a potentially wide range of applications not only to framework silicates glasses, but to more complex multicomponent oxide glasses where the extent of disorder is complicated by the formation of ^{14}B and even to disordered crystalline phases such as zeolites and clay minerals.

Acknowledgments—This project was supported by a Stanford Graduate Fellowship and by NSF grant DMR9802072. We thank Dr. S. Wang for helpful discussion, two anonymous reviewers, and Prof. Ghiorso for helpful comments on the manuscript.

Associate editor: M. S. Ghiorso

REFERENCES

- Baltisberger J. H., Xu Z., Stebbins J. F., Wang S., and Pines A. (1996) Triple-quantum two-dimensional ^{27}Al magic-angle spinning nuclear magnetic resonance spectroscopic study of aluminosilicate and aluminate crystals and glasses. *J. Am. Chem. Soc.* **118**, 7209–7214.
- Bouhifd M. A., Sipp A., and Richet P. (1999) Heat capacity, viscosity, and configurational entropy of alkali titanosilicate melts. *Geochim. Cosmochim. Acta* **63**, 2429–2437.
- Charles R. J. and Wagstaff F. E. (1968) Metastable immiscibility in the $\text{B}_2\text{O}_3\text{-SiO}_2$ system. *J. Am. Ceramic Soc.* **51**, 16.
- Dell W. J., Bray P. J., and Xiao S. Z. (1983) ^{11}B NMR studies and structural modeling of $\text{Na}_2\text{O-B}_2\text{O}_3\text{-SiO}_2$ glasses of high soda content. *J. Non-Cryst. Solids* **58**, 1–16.
- Engelhardt G. and Michel D. (1987) *High-Resolution Solid-State NMR of Silicates and Zeolites*. Wiley.
- Hervig R. L. and Navrotsky A. (1985) Thermochemistry of sodium borosilicate glasses. *J. Am. Ceramic Soc.* **68**, 314–319.
- Hwang S. J., Fernandez C., Amoureux J. P., Cho J., Martin S. W., and Pruski M. (1997) Quantitative study of the short range order in B_2O_3 and B_2S_3 by MAS and two-dimensional triple-quantum MAS B-11 NMR. *Sol. St. NMR* **8**, 109–121.
- Lee S. K. and Stebbins J. F. (1999) The degree of aluminum avoidance in aluminosilicate glasses. *Am. Mineral.* **84**, 937–945.
- Lee S. K. and Stebbins J. F. (2000a) Al-O-Al and Si-O-Si sites in framework aluminosilicate glasses with $\text{Si/Al} = 1$: Quantification of framework disorder. *J. Non-Cryst. Solids* **270**, 260–264.
- Lee S. K. and Stebbins J. F. (2000b) The structure of aluminosilicate glasses: High-resolution ^{17}O and ^{27}Al MAS and 3QMAS NMR study. *J. Phys. Chem. B* **104**, 4091–4100.
- Lee S. K., Musgrave C. B., Zhao P., and Stebbins J. F. (in press) Topological disorder and reactivity of borosilicate glasses: Quantum chemical calculations and ^{17}O and ^{11}B NMR study. *J. Phys. Chem. B*.
- Martens R. and Müller-Warmuth W. (2000) Structural groups and their mixing in borosilicate glasses of various compositions: an NMR study. *J. Non-Cryst. Solids* **265**, 167–175.
- Mysen B. (1998) Transport and configurational properties of silicate melts: Relationship to melt structure at magmatic temperatures. *Phys. Earth Planet. Int.* **107**, 23–32.
- Mysen B. O., Virgo D., and Seifert F. A. (1982) The structure of silicate melts: Implications for chemical and physical properties of natural magma. *Rev. Geophys. Space Phys.* **20**, 353–383.
- Navrotsky A., Peraudeau G., McMillan P., and Coutures J. P. (1982) A thermochemical study of glasses and crystals along the joins silica-calcium aluminate and silica-sodium aluminate. *Geochim. Cosmochim. Acta* **46**, 2039–2047.
- Petkov V., Gerber T., and Himmel B. (1998) Atomic ordering in $\text{Ca}_{x/2}\text{Al}_x\text{Si}_{1-x}\text{O}_2$ glasses ($X = 0, 0.34, 0.5, 0.68$) by energy-dispersive X-ray-diffraction. *Phys. Rev. B* **58**, 11982–11989.
- Petkov V., Billinge S. J. L., Shastri S. D., and Himmel B. (2000) Polyhedral units and network connectivity in calcium aluminosilicate glasses from high-energy X-ray diffraction. *Phys. Rev. Lett.* **85**, 3436–3439.
- Porai-Koshits, E. A. and Wright, A. C. (1996) Some paradoxes of borate glasses and melts. In (eds. A. C. Wright, S. A. Feller and A. C. Hannon), *Borate glasses, crystals and melts*, p. 51–62. Society of glass technology, Abingdon, UK.
- Richet P., Bouhifd M. A., Courtial P., and Tequi C. (1997) Configurational heat capacity and entropy of borosilicate melts. *J. Non-Cryst. Solids* **211**, 271–280.
- Sorarú G. D., Dallabona N., Gervais C., and Babonneau F. (1999) Organically modified $\text{SiO}_2\text{-B}_2\text{O}_3$ gels displaying a high content of borosiloxane (=B-O-Si) bonds. *Chem. Mater.* **11**, 910–919.
- Stebbins J. F. and Xu Z. (1997) NMR evidence for excess non-bridging oxygen in aluminosilicate glass. *Nature* **390**, 60–62.
- Stebbins J. F., Lee S. K., and Oglesby J. V. (1999a) Al-O-Al oxygen sites in crystalline aluminates and aluminosilicate glasses: High-resolution oxygen-17 NMR results. *Am. Mineral.* **84**, 983–986.
- Stebbins J. F., Zhao P., Lee S. K., and Cheng X. (1999b) Reactive Al-O-Al sites in a natural zeolite: Triple-quantum oxygen-17 nuclear magnetic resonance. *Am. Mineral.* **84**, 1680–1684.
- Wang S. and Stebbins J. F. (1998) On the structure of borosilicate glasses: A triple-quantum magic-angle spinning ^{17}O NMR study. *J. Non-Cryst. Solids* **231**, 286–290.
- Wright A. C., Feller S. A., and Hannon A. C. (1996) *Borate glasses, crystals, and melts*, Society of glass technology, Sheffield, UK, p. 570.
- Youngman R. E., Haubrich S. T., Zwanziger J. W., Janicke M. T., and Chmelka B. F. (1995) Short- and intermediate-range structural ordering in glassy boron oxide. *Science* **269**, 1416–1420.